Applied Mechanics and Materials Vols. 373-375 (2013) pp 770-784
© (2013) Trans Tech Publications, Switzerland
doi:10.4028/www.scientific.net/AMM.373-375.770

System Identification of a Six-Legged Semisubmersible Subjected to Wave Loads through Frequency Domain Analysis

Guo Zheng Yew[1, a], Eu Shawn Lim[1,b], Mohd Shahir Liew[1,c] and Cheng Yee Ng[1,d]

[1]Civil Engineering Department, Universiti Teknologi PETRONAS, Bandar Seri Iskandar, 31750, Tronoh, Perak, Malaysia.

[a]henry.yew88@gmail.com, [b]shahir_liew@petronas.com.my, [c]lim.eu.shawn@gmail.com, [d]carrol.ng82@gmail.com

Keywords: Transfer function, frequency domain, semisubmersible, wave loads, floating offshore structures, autocorrelation function, autospectral density function, random vibrations

Abstract. Sea state conditions such as wind, wave and current vary in different ocean waters. Two similar offshore structures installed in two different ocean regions will yield different responses. Determining the transfer function of the structure is a system identification exercise that yields the structural response and behaviour given any sea state condition. The transfer function can be determined using available measured sea state data and structural response data. In this paper, a six-legged semisubmersible physical model is developed to a scale of 1:100 and is tested in a wave tank to measure its responses due to simulated random wave loads. The transfer functions of the semisubmersible model are then determined using the measured responses and the measured wave heights.

Introduction

A semisubmersible, as shown in Fig. 1 [1], is a floating offshore structure that is usually employed in deepwater environments. Mooring lines are installed on the semisubmersible and tied to the seabed to resist the structure against excessive movements due to the action of wind, waves and current.

Fig. 1: A semisubmersible

A floating structure subjected to sea state loads can respond in six different degrees of freedom (DOFs) corresponding to three translational movements and three rotational movements. The DOFs include: surge, sway, heave, pitch, roll and yaw. The surge DOF is defined as the translational motion parallel to the direction of the force or the excitation. Fig. 2 illustrates the six DOFs.

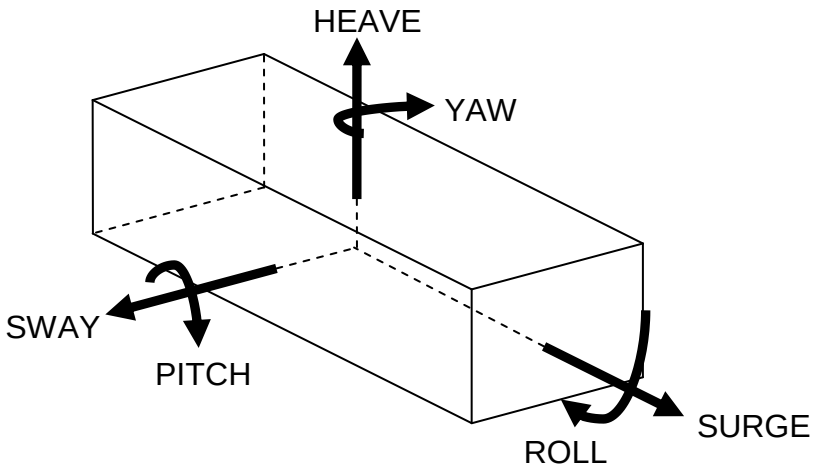

Fig. 2: The six DOFs of a floating structure

As different ocean waters have varying sea state conditions, a particular semisubmersible is expected to behave and respond differently in each oceanic region. In order to analyse the response of the structure due to environmental loads, one method is to install sensors such as accelerometers, wave probes and anemometers to measure and record sea state conditions as well as structural responses. However, to conduct such an exercise for a particular structure installed in different geographical regions is impractical due to the sheer physical and financial scale of the project.

Alternatively, the measured sea state data and structural response data in one geographical location can be used to derive the transfer function of the structure. Once the transfer function is known, the structural responses can be determined corresponding to various environmental loads. This is a system identification exercise which enables the structural behaviour and responses to be analysed mathematically regardless of geographical location and sea state conditions.

This paper provides the framework to obtain the transfer function of a semisubmersible model (developed to a scale of 1:100) by subjecting it to simulated random waves by wave generators in a wave tank; the wave heights and the structural responses in all DOFs are measured and recorded. The experimental setup will be outlined, and the mathematical and statistical formulations that lead to the computation of the transfer function will be explained in detail.

Literature Review

Time Series. A time series is a sequence of observations measured and recorded sequentially, with a constant time interval between any two adjacent observations [2]. A time series can give an indication of whether a particular process is deterministic or random. A deterministic process implies that the time series can be modelled or represented analytically by a mathematical expression. If a process is deterministic, then the characteristics of the process can be accurately determined through mathematical relationships.

In most civil engineering applications, however, the measured structural responses and meteorological data cannot be represented easily by a mathematical model, but can be analysed statistically in terms of mean, variance and correlation. Such nondeterministic processes are deemed as random (or stochastic), and they are the focus of this paper. Fig. 3 shows an example of a time history for a random process (structural response) measured by an accelerometer.

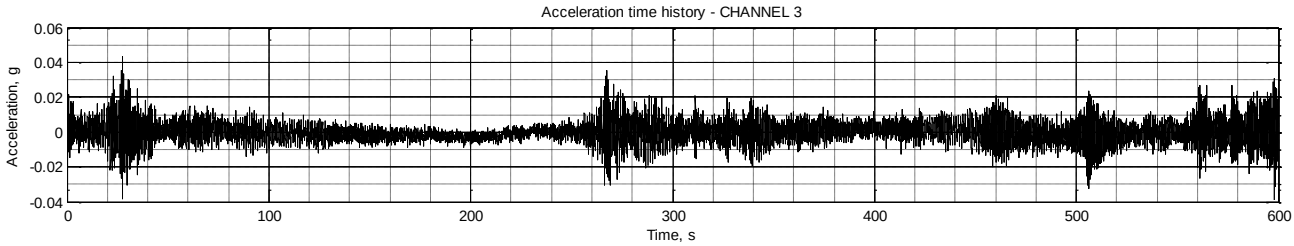

Fig. 3: Time series of a random process

A random process can be classified as stationary or nonstationary. While most random processes are nonstationary, they are usually transformed to stationary processes (by first differencing) or initially assumed to be weakly stationary to simplify the analysis of data. A weakly stationary process has mean and variance values that do not vary with time.

Autocorrelation Function. Correlation portrays the linear relationship and dependence between two variables *x* and *y*. The autocorrelation function reveals how the correlation between the time series *x(t)* and a lagged version of itself *x(t + τ)* – where *τ* is the lag number – changes [2]. If the entire time series is correlated with itself, the autocorrelation function will yield unity, indicating a perfect correlation. As the lag *τ* increases, the autocorrelation may eventually reach zero, at which point the original time series and the lagged time series are said to be uncorrelated at lag *τ*.

For a random process denoted by *{X(t)}*, the autocorrelation function is defined as [3]:

$$\phi_{XX}(t,s) = E[X(t)X(s)] = \int_{-\infty}^{\infty}\int_{-\infty}^{\infty} u\, v\, p_{X(t)X(s)}(u,v)du\, dv \tag{1}$$

where $p_{X(t)X(s)}(u,v)$ is the joint probability distribution function of *X(t)* and *X(s)*. If $s = t + \tau$, then the autocorrelation function can be expressed as a function of the lag *τ* [3, 4]:

$$R_{XX}(\tau) = \phi_{XX}(t, t+\tau) = E[X(t)X(t+\tau)] = \int_{-\infty}^{\infty}\int_{-\infty}^{\infty} u\, v\, p_{X(t)X(t+\tau)}(u,v)du\, dv \tag{2}$$

Eq. 1 and Eq. 2 are analytical expressions of the autocorrelation function, and can be computed easily provided that the joint probability distribution function is known. Both equations require that we have time series of infinite lengths, but time series observations are always of finite length. Therefore, the autocorrelation function for a finite number of observations is, at best, an estimate. The expression that gives the most satisfactory estimate of the autocorrelation function is [2]:

$$\hat{R}_{XX}(\tau) = \frac{c(\tau)}{c(0)} \tag{3}$$

where

$$c(\tau) = \frac{1}{N}\sum_{t=1}^{N-\tau}[x(t) - \bar{x}][x(t+\tau) - \bar{x}] \tag{4}$$

N represents the sample size of the time series observations and $\bar{x}$ is the sample mean of *{X(t)}*. Eq. 3 simply indicates that the autocorrelation function at lag *τ* is simply the ratio of the autocovariance at lag *τ* to the sample variance *c(0)*.

The autocorrelation function can yield important information with regards to the stationarity of a random process *{X(t)}*. For a random process to be stationary, the autocorrelation function must only depend on lag *τ* and cannot change with time *t*. An autocorrelation function with a constant mean and which decays rapidly are indication of a weakly stationary process [2, 5, 6]. A weakly stationary process will allow simplifications of various time series analysis expressions, and it is an important criterion that must be fulfilled prior to obtaining the autospectral density function.

Autospectral Density Function. The autospectral density function shows the decomposition of a random process into its frequency components which helps to identify periodicities in the process. It can be derived from the Fourier transform of the autocorrelation function given as [4]:

$$S_{XX}(f) = \int_{-\infty}^{\infty} R_{XX}(\tau) e^{-i2\pi f\tau} d\tau \quad (5)$$

where $i = \sqrt{-1}$.

For a time series of finite lengths, however, an estimate of the autospectral density function can be obtained through discrete Fourier transforms of the autocorrelation function based on Eq. 5. Alternatively, with the advent of the Fast Fourier Transform, the autospectral density function can be estimated from a time history ensemble that has been divided into n_d number of distinct and disjoint subrecords – each of length T – and then averaging the results to obtain the spectral estimate given by [7]:

$$\hat{G}_{XX}(f) = \frac{2}{n_d T} \sum_{i=1}^{n_d} |X_i(f,T)|^2 \quad (6)$$

where $X_i(f, T)$ is the discrete Fourier transform of $\{X(t)\}$, expressed mathematically as:

$$X_i(f,T) = \int_0^T x_i(\tau) e^{-i2\pi f\tau} d\tau \quad (7)$$

Transfer Function. A linear time-invariant system with excitation $f(t)$ and response $x(t)$, or their Fourier transform counterparts, $\tilde{F}(\omega)$ and $\tilde{X}(\omega)$, can be described by a transfer function, $H_x(\omega)$, as shown in Fig. 4.

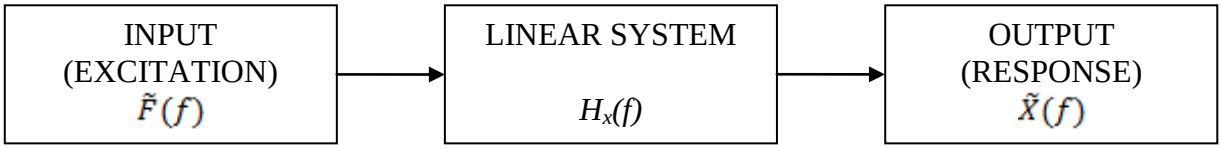

Fig. 4: Schematic describing a linear time-invariant system

A random excitation $\{F(t)\}$ will generate a random structural response $\{X(t)\}$, and the autospectral density function for each of the random process can be obtained. With the two autospectral density functions known, the transfer function for a linear time-invariant system can be computed using the expression given by [3]:

$$S_{XX}(f) = |H_x(f)|^2 S_{FF} \quad (8)$$

Application of Sea Spectra for Wave Generation. For the purpose of the wave tank tests, the wave parameters were modelled after existing sea spectra that have already been established for offshore design. This is often the most suitable method for wave generation as it is able to better simulate the stochastic conditions of an actual sea state, whereby the sea waves are thought to be consisting of a finite sum of Fourier waves. This in turn would be represented in the frequency domain as a distribution of spectral energy over a range of wave frequencies. The alternative method to this would be the generation of regular waves upon the model. While this is much easier to simulate and predict resultant responses, it is highly unrepresentative of the stochastic sea states [8].

The initial assumption for this wave tank test was to replicate the sea states to that of a fetch limited sea. This would indicate limitation in the assumptions of two particular parameters, namely fetch length and fetch duration. As such, it was proposed that the Joint North Sea Wave Project

(JONSWAP) spectrum be utilized to model the required sea states as the JONSWAP spectrum was designed with the initial assumption of fetch limitation [9, 10]. The characteristic of fetch limitation tends to manifest itself in the spectrum as a higher a narrower peak compared to that of a fully developed sea, thus indicating spectral concentration towards a smaller range of frequencies that is usually seen in fetch limited regions [11]. Contrary to the abbreviation that JONSWAP spectrum stands for, it can be modified to suit the localities of other regions through the alteration of the gamma factor, γ also known as the spectral peak factor. The JONSWAP empirical formula is given by [12]:

$$S(\omega) = \alpha g^2 \omega^{-5} e^{\left[-1.25\left(\frac{\omega}{\omega_0}\right)^{-4}\right]} \gamma^{e^{\left[\frac{-(\omega-\omega_0)^2}{2\tau^2\omega_0^2}\right]}} \quad (9)$$

From Eq. 9, the JONSWAP spectrum is observed to be a two-parameter spectrum as a function of ω_0 and γ, whereby ω_0 is defined as the dominant or fundamental frequency of the sea spectra and γ is defined as the peak factor of the spectrum governed by the relationship of significant wave height H_s and peak period T_p of the modelled sea state [12]. Other spectral parameters are considered to be sufficiently stable to be considered as constants based on holding assumptions of the JONSWAP spectrum such as the zeroth factor α and shape parameter τ. Ideally, wave data originating from the region of concern are preferred so that a spectral analysis can be performed to determine site-specific gamma values empirically by fitting the zeroth moment z_0 of the spectrum or using the measured H_s and T_p. Fig. 5 displays the relationship of the γ factor on the spectral shape, indicating fetch effects [12].

In the case that the wave generation is generic and independent of regional modelling, the γ factor is set to 3.3 which is representative of North Sea conditions.

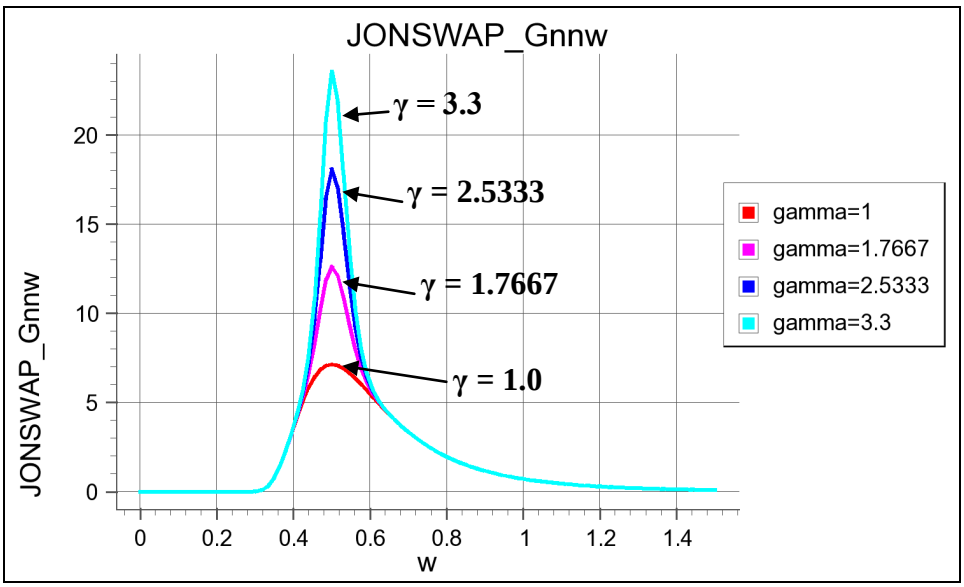

Fig. 5: Effect of γ on the spectral shape

Experimental Setup

A semisubmersible model was developed to a scale of 1:100. This is to enable the placement and modelling of the structure within the wave tank's limitations. Fig. 6 shows a test submersible model. Figures 7 and 8 show the dimensions of the model, all in millimetres. Three wave probes were placed to measure the local wave heights in the tank.

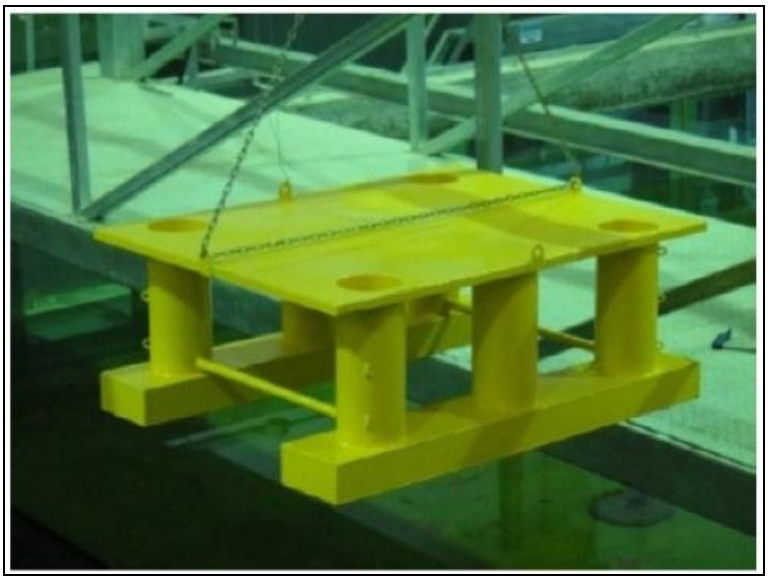

Fig.6: Scaled-down model of the semisubmersible

The test model was subjected to unidirectional random waves generated using the JONSWAP spectrum, with the experimental layout as shown in Fig. 9. Table 1 shows the wave parameters scaled down by using Froude modelling. The wave generation parameters from the table are then translated into the frequency domain based on the generated time series from the wave probes. Resultant from the Fourier transform of the time series, the sea spectra are obtained and they serve as the inputs (excitation) to the system.

The generated wave height and the structural responses were then measured and recorded. The autospectral density functions of the excitation and the responses were quantified and the transfer functions were then determined.

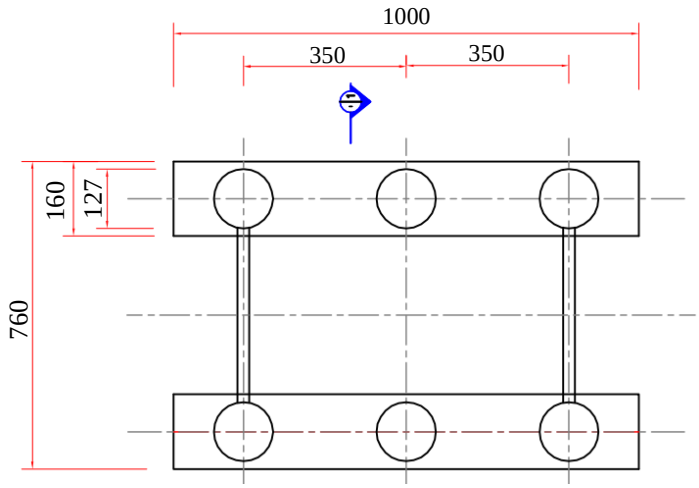

Fig. 7: Dimensions of the semisubmersible model (plan view)

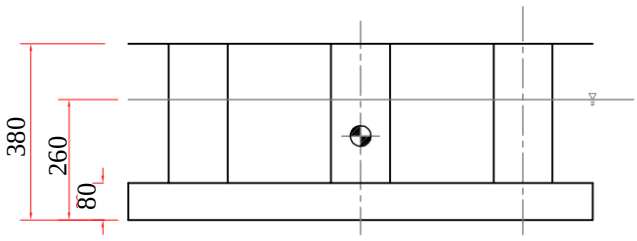

Fig. 8: Leg dimensions of the semisubmersible model (side view)

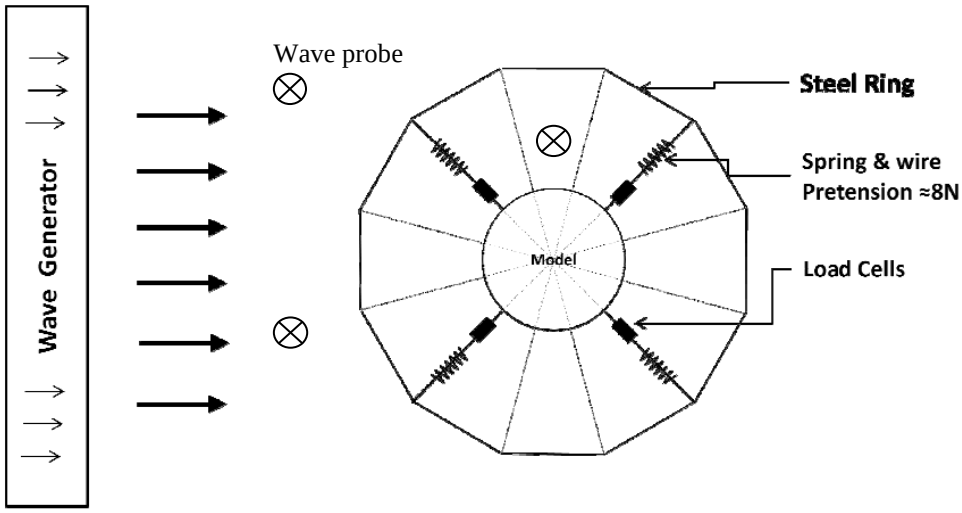

Fig. 9: Plan view of the experimental setup

Table 1: Wave modelling parameters of the sea states

Test No.	Wave Frequency [Hz]	Wave Period [s]	Significant wave height [m]
RD2	0.71	1.40	0.06
RD3	1.00	1.00	0.05
RD4	0.83	1.20	0.07

Assumptions and Limitations

In the due course of modelling the wave parameters, several assumptions and limitations were established in order to better interpret certain phenomena in the results presented herein. These modelling limitations manifest themselves due to the physical setup of the wave tank, similitude laws of scaling and the ability of the wave generators to model a stochastic process.

Due to testing in a wave tank, the structural model was left susceptible to the effects of side wall currents. Experiments tend to suffer primarily due to the finite width of the wave tanks and the effects of waves on the side boundaries on the hydrodynamic processes. Approaching waves create longshore currents that result in rip currents along the sidewalls, and on the long run it creates large-scale circulation within the wave tank [13].

Due to the scale of the model, which was capped at 1:100, the testing parameters are subjected to the laws of similitude. This is to ensure that the parameters are scaled down appropriately to represent full-scale conditions; while some scales are linearly related, some others are related by a nonlinear coefficient. Mass and displacement are linearly related while time factors are computed as the square root of the scale factor, or in our case, the square root of 100. Even with similitude laws in place, experimental anomalies such as small shifts in mass distribution of model structure and angle of wave direction compared to a full-scale model is very likely to result in amplified errors when scaled back. In addition, physical characteristics of the structure such as material stiffness cannot be scaled down and therefore must be stated the initial assumption of this test. Furthermore, it is important to note that the generation of waves in the wave tank are at best weakly stationary in nature. This is due to the algorithm utilized by the wave generators which uses the sum of Fourier waves based on the specified sea spectra to generate the spectral distribution; they are periodic and stationary in nature. The actual sea states, however, are natural random processes and therefore are fundamentally nonstationary [11].

Results and Discussion

As the experimental setup is carried out based on a zero-degree wave heading, it is anticipated that the structure should theoretically not yield any responses in the sway, roll and yaw degrees of freedom. However due to factors such as sidewall effects, efficiency of wave attenuators and issues related to human precision such as perfect orthogonal placement of the structure in the wave tank with respect to the wave heading, it is anticipated that there would be some responses in the sway, roll and yaw degrees of freedom.

Analysis of System Inputs. In the experimental setup, the waves were generated based on a distribution of waves as described based on the JONSWAP spectrum empirical formula given by Eq. 9. Fig. 10 shows the autospectral density functions for the three different generated waves: RD2, RD3 and RD4.

The spectrum is seen to concur very closely with experimental setup values whereby RD2 test obtains 0.65Hz, RD3 at 0.80HZ and RD4 at 1.10Hz peak frequencies. There is lower spectral content present around the peak frequencies and this is consistent with the generation of the JONSWAP spectrum wave. Peak frequency magnitudes theoretically should yield lower magnitudes at higher frequencies and this characteristic is present in the experimental results.

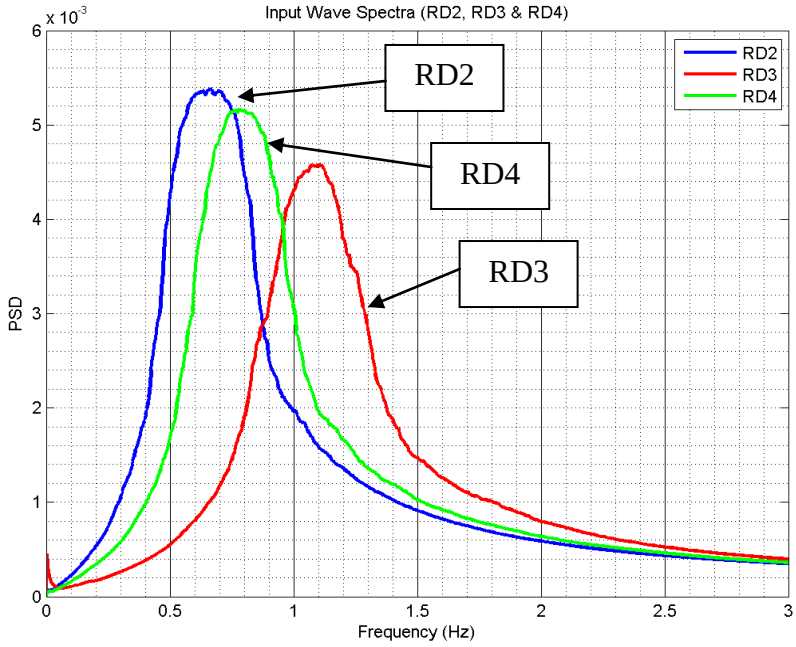

Fig. 10: Autospectral density functions for waves RD2, RD3 and RD4

Stationarity of Semisubmersible Responses. Stationarity checks are performed to ensure that the time series ensemble can undergo the frequency domain analysis. These are verified through the autocorrelation function plots of the time series. Figs. 11, 12 and 13 show the autocorrelation function plots for heave, surge and pitch DOFs respectively due to the different wave inputs.

Generally the autocorrelation plots indicate a weakly stationary nature of the time series from tests RD2, RD3 and RD4. This is indicated by the autocorrelation plots having a relatively fast decay with respect to lag values. Based on the plots, sinusoidal characteristics can be observed indicating a periodic effect of waves being omnipresent throughout the experiment. In addition, multiple sinusoids of different frequencies are observed in the autocorrelation plot, indicating the distribution of wave frequencies characteristic to the JONSWAP spectrum.

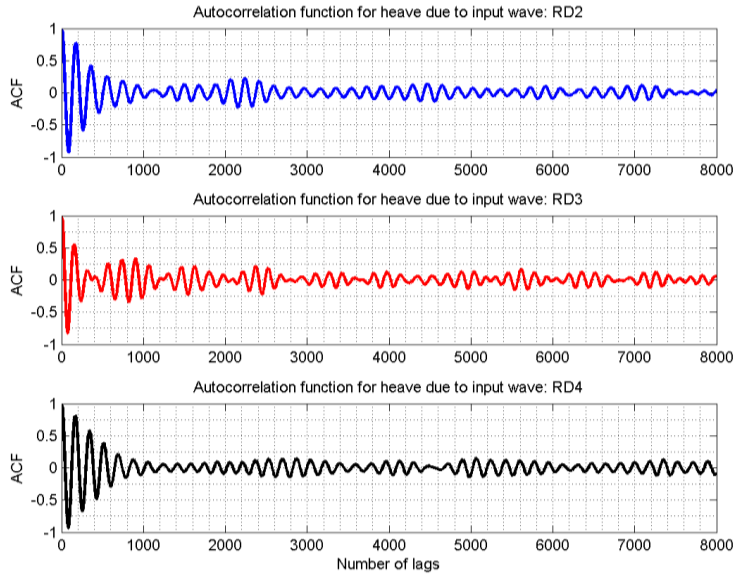

Fig. 11: Autocorrelation function plots for the heave DOF

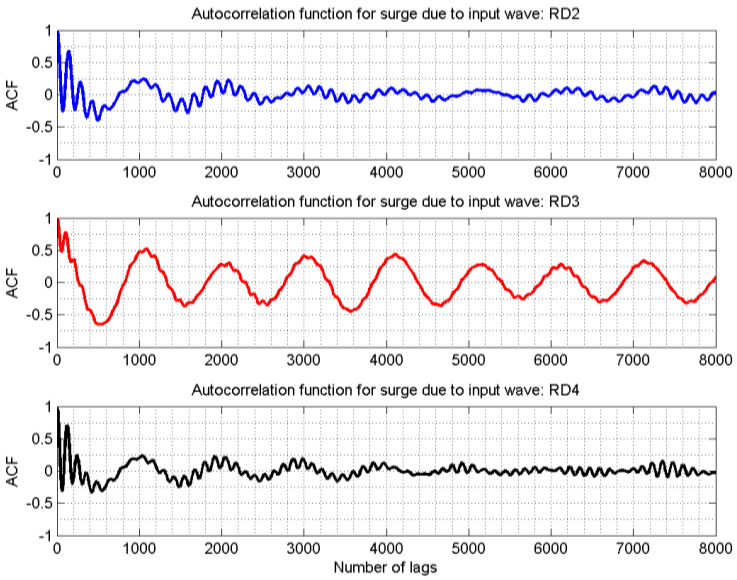

Fig. 12: Autocorrelation function plots for the surge DOF

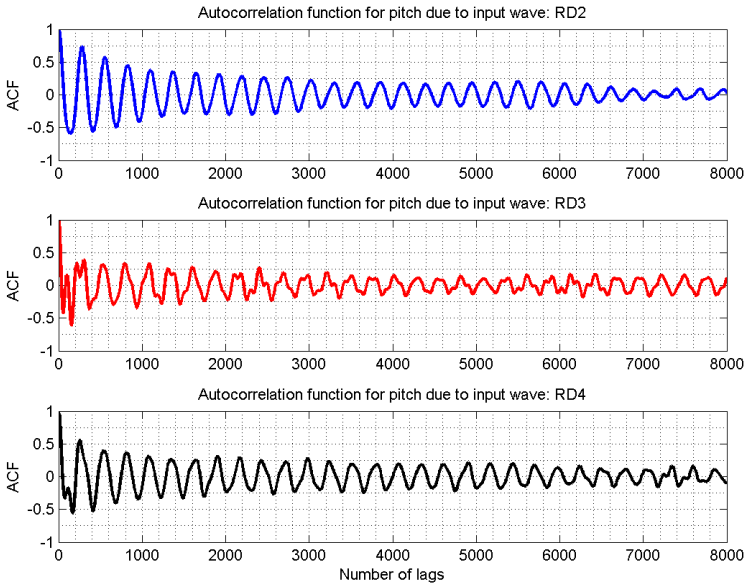

Fig. 13: Autocorrelation function plots for the pitch DOF

Response Autospectral Density Functions. The Fourier transform of the autocorrelation functions would yield the response autospectral density functions as defined by Eq. 5. Figs. 14 to 16 show the autospectral density functions for the translational DOFs, while Figs. 17 to 19 show the autospectral density functions for the rotational DOFs.

Table 2 summarises the peak response frequency that appeared consistently in the autospectral plots for all three wave inputs, as well as the secondary peak frequencies which correspond to the forcing frequency.

Table 2: Peak response frequencies for each DOF and secondary frequencies for each input wave

Degree of Freedom	*Peak response frequency [Hz]*	*Remarks*
Heave	0.46	
Surge	0.10	Anticipated due to symmetry of the structure
Sway	0.10	
Pitch	0.32	Anticipated due to symmetry of the structure
Roll	0.32	
Yaw	0.22	
Secondary peaks corresponding to the forcing frequency of the waves		
Input Wave	*Structural response frequency [Hz]*	*Remarks*
RD2	0.67	Corresponds closely to the dominant wave frequency
RD3	0.90 to 1.00	Low spectral magnitude as forcing frequency is spaced farther away from fundamental frequencies of structure
RD4	0.83	Corresponds to the dominant wave frequency

Peaks are also observed consistently at 0.70 Hz in the heave, surge and pitch DOFs when the structure was excited by input waves RD2 and RD4. This could correspond to the natural frequency of the mooring lines which were attached to the semisubmersible model. The resonating motions of the mooring lines could generate motions in the model, thus contributing to the spectral energy content.

Transfer Function. Interpretations of the response spectrum are akin to performing modal analysis of a structure. It is an output-based only analysis and is analogous to a black box system, where the spectral peaks cannot be clearly identified until further information is verified and fed into the system. As such, transfer functions enable the identification of responses that is characteristic to the structure, thus separating spectral peaks belonging to the forcing frequency from those corresponding to the natural frequencies of the structure. Figs. 20 to 22 show the transfer function plots for the translational DOFs, while Figs. 23 to 25 show the transfer function plots for the rotational DOFs.

Table 3 summarises the first dominant frequencies that are observed from the transfer function plots.

Table 3: First dominant frequencies obtained from the transfer function plots

Degree of Freedom	*First dominant frequency [Hz]*	*Remarks*
Heave	0.46	Corresponds to the first mode of vibration
Surge	0.10	
Sway	0.10	
Pitch	0.30	
Roll	0.30	
Yaw	0.22	

A secondary peak observed at 0.70 Hz in the transfer function plots for all DOFs except the yaw DOF again suggests that the contribution could have originated from the vibration of the mooring lines.

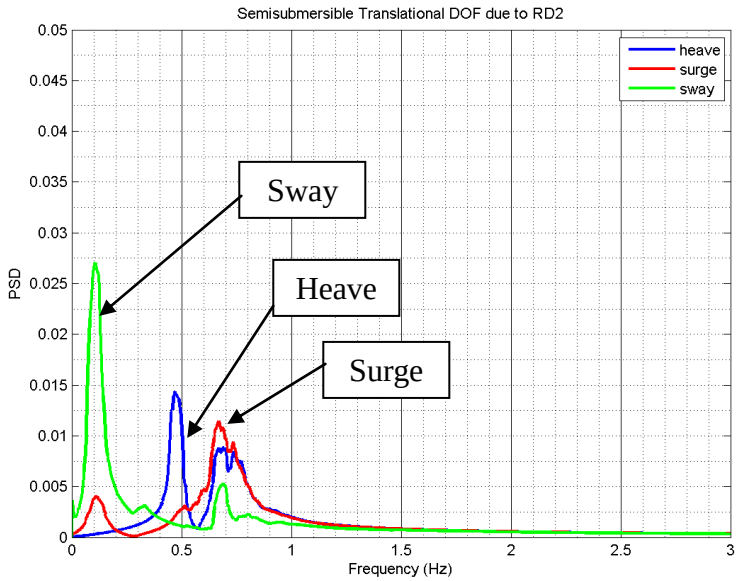

Fig. 14: Response autospectral density functions for translational DOFs due to input wave: RD2

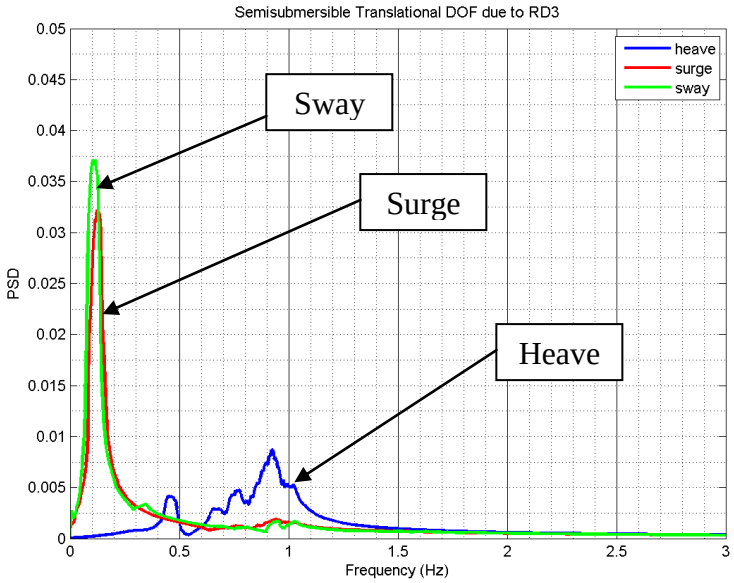

Fig. 15: Response autospectral density functions for translational DOFs due to input wave: RD3

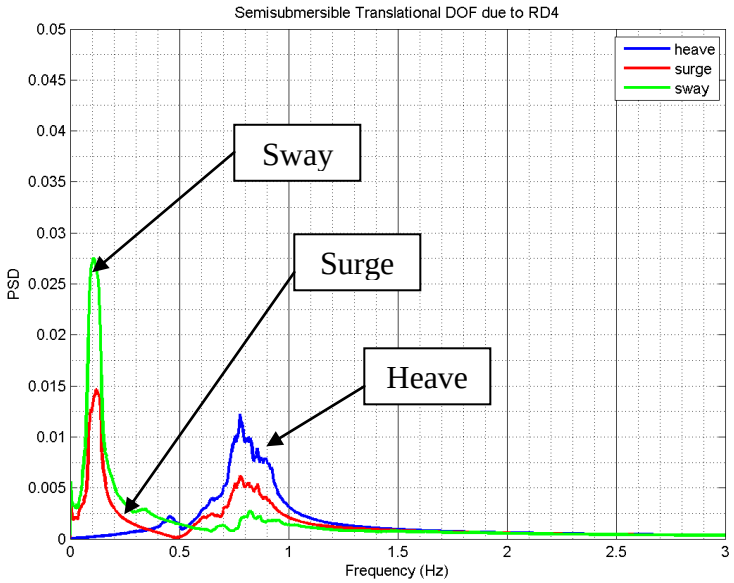

Fig. 16: Response autospectral density functions for translational DOFs due to input wave: RD4

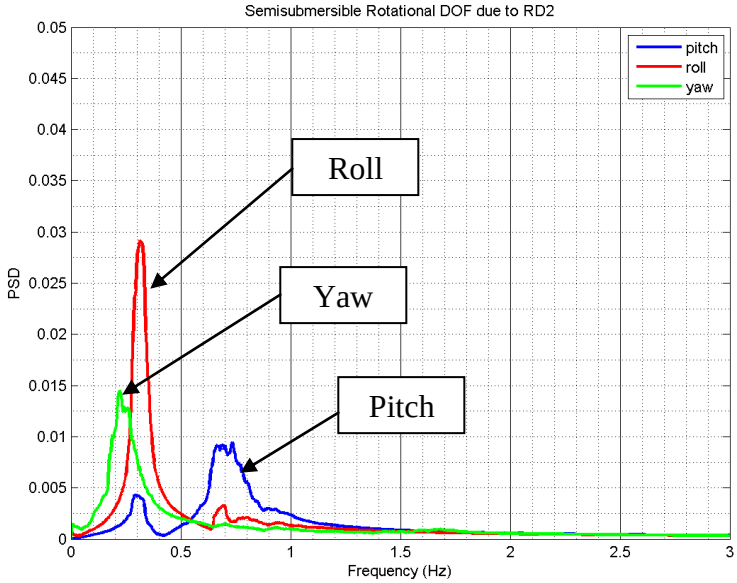

Fig. 17: Response autospectral density functions for rotational DOFs due to input wave: RD2

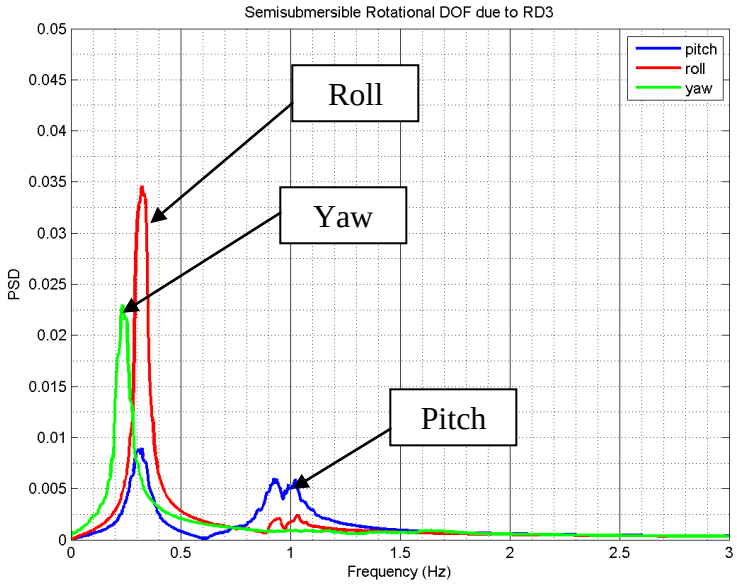

Fig. 18: Response autospectral density functions for rotational DOFs due to input wave: RD3

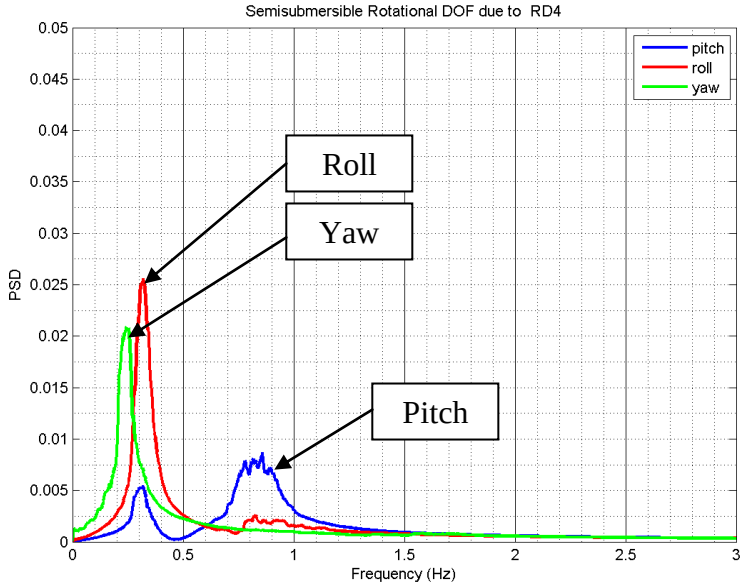

Fig. 19: Response autospectral density functions for rotational DOFs due to input wave: RD4

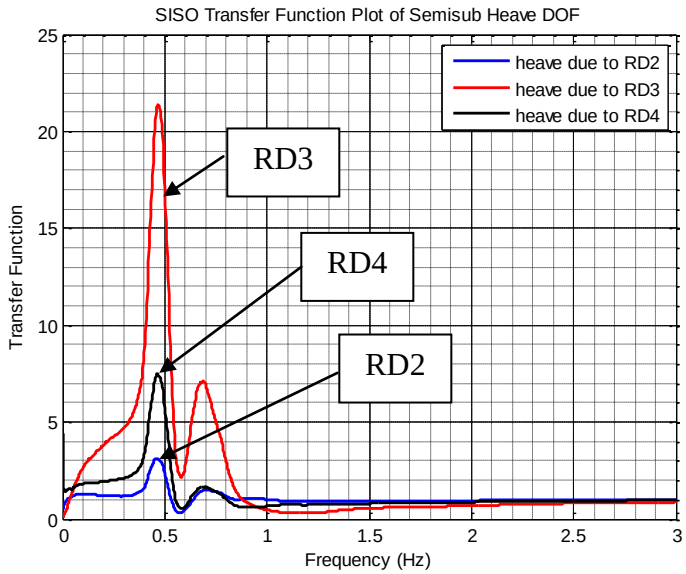

Fig. 20: Transfer function plots for the heave DOF

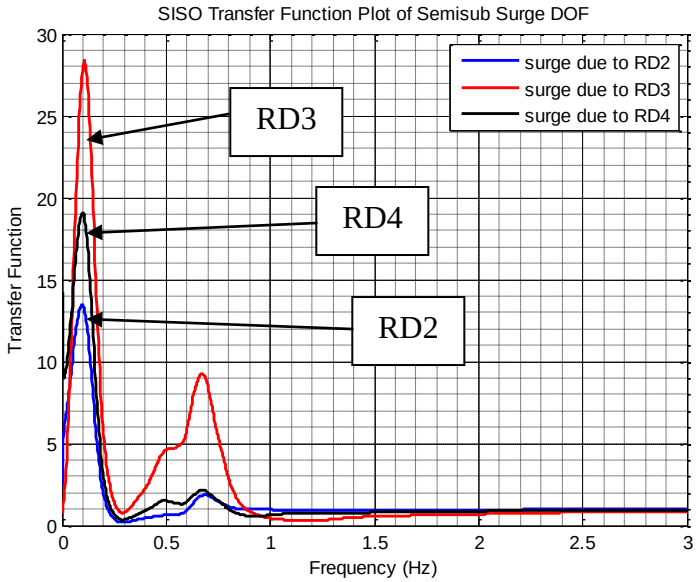

Fig. 21: Transfer function plots for the surge DOF

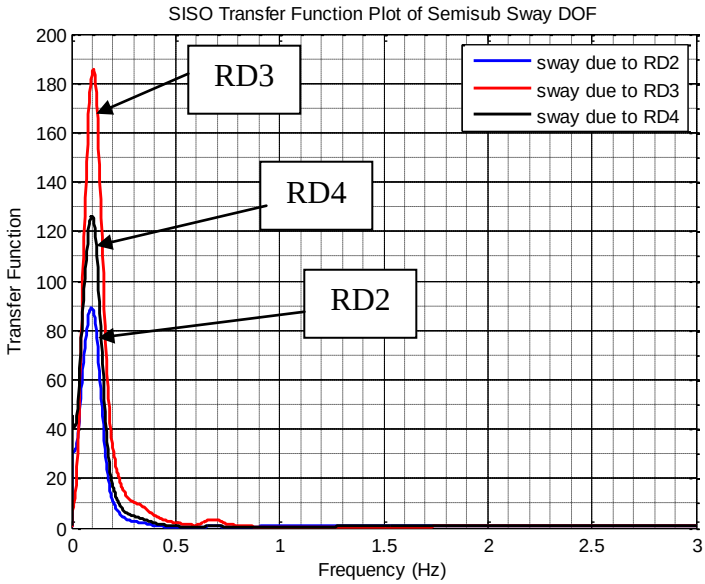

Fig. 22: Transfer function plots for the sway DOF

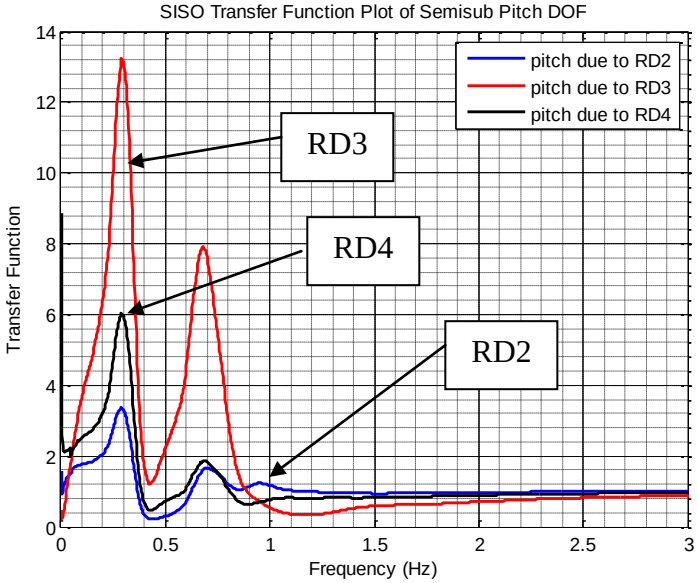

Fig. 23: Transfer function plots for the pitch DOF

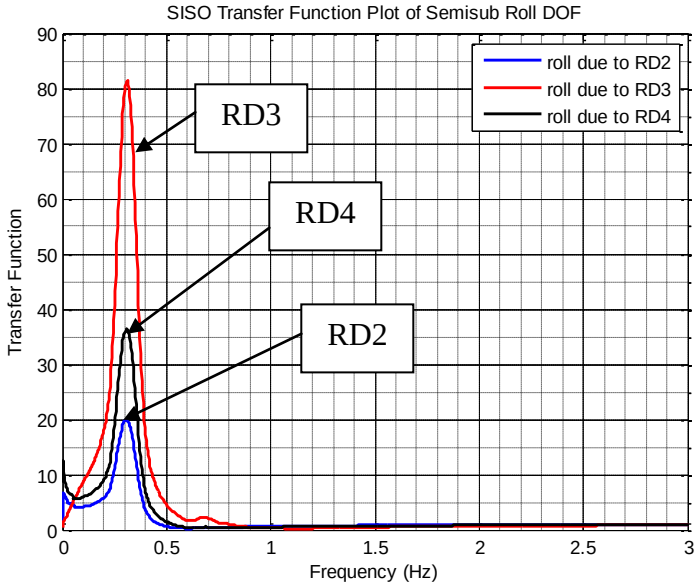

Fig. 24: Transfer function plots for the roll DOF

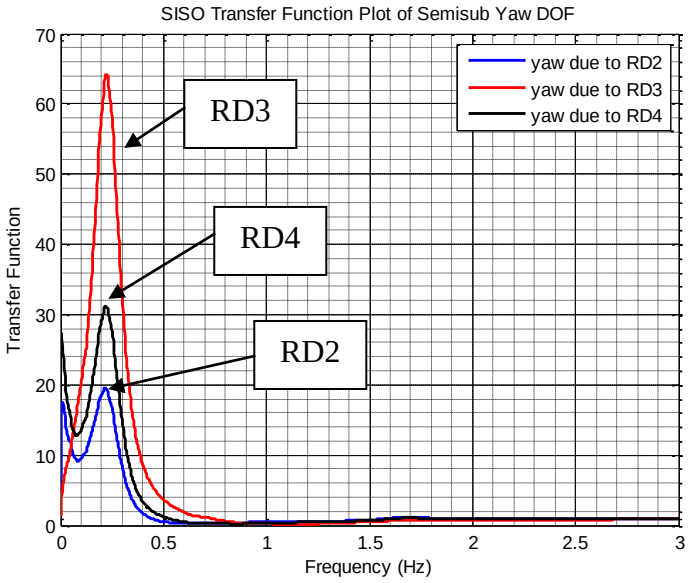

Fig. 25: Transfer function plots for the yaw DOF

Conclusion

A framework to determine the transfer functions of a semisubmersible model subjected to wave loads was presented in this paper. The transfer functions obtained were able to provide information on the natural frequencies of the semisubmersible model. The transfer functions identified the natural frequencies of the semisubmersible model to be 0.10 Hz (surge and sway DOFs), 0.22 Hz (yaw DOF) 0.30 Hz (pitch and roll DOFs) and 0.46 Hz (heave DOF).

Recommendation

Full-scale testing on existing semisubmersibles should be conducted to obtain data which could be used to verify the results obtained from the scaled-down model tests. The same framework on obtaining the transfer function can be employed and then results are compared to determine the level of agreement between the model test and the full-scale test.

References

[1] Graphic obtained from www.safety4sea.com/images/media/2011.7.8-Transocean%20Ltd..jpg

[2] G.E.P. Box, G.M. Jenkins and G.C. Reinsel, in: *Time Series Analysis: Forecasting and Control*, John Wiley & Sons, Hoboken, NJ (2008)

[3] L.D. Lutes and S. Sarkani, in: *Random Vibrations: Analysis of Structural and Mechanical Systems*, Elsevier Butterworth-Heinemann, Burlington, MA (2004)

[4] J.S. Bendat and A.G. Piersol, in: *Engineering Applications of Correlation and Spectral Analysis*, John Wiley & Sons, New York, NY (1993)

[5] R.E. Challis and R.I. Kitney, in: *Biomedical Signal Processing (in Four Parts) – Part 1*, Medical & Biological Engineering & Computing, Vol. 28 (1990), pp. 509-524

[6] B.L. Bowerman and R.T. O'Connell, in: *Time Series and Forecasting*, Duxbury Press, North Scituate, MA (1979)

[7] J.S. Bendat and A.G. Piersol, in: *Random Data: Analysis and Measurement Procedures*, John Wiley & Sons, Hoboken, NJ (2010)

[8] W. Michel, in: *Sea Spectra Revisited*, Marine Technology, Vol. 36 (1999), No. 4, pp. 221-227

[9] S. Chakrabarti, in: *Handbook of Offshore Engineering (Vol. 1)*, Offshore Structure Analysis, Plainfield, IL (2005)

[10] W.J. Pierson, in: *A Proposed Spectral Form for Fully Developed Wind Seas based on the Similarity Theory of S.A. Kitaigorodskii*, Journal of Geophysical Research (1964), pp. 5181-5190

[11] H.L. Holthuijsen, in: *Waves in Oceanic and Coastal Waters*, Delft University of Technology, UNESCO-IHE: Cambridge University Press (2007)

[12] S. Chakrabarti, in: *Hydrodynamics of Offshore Structures*, WIT Press, Southampton, UK (1987)

[13] S.A. Hughes, in: *Physical Models and Laboratory Techniques in Coastal Engineering*, World Scientific (1993)